Original

Cavicchia, L.; Storch, H.v.; Gualdi, S.:

Mediterranean Tropical-Like Cyclones in Present and Future Climate

In: Journal of Climate (2014) AMS

DOI: 10.1175/JCLI-D-14-00339.1

Mediterranean Tropical-Like Cyclones in Present and Future Climate

LEONE CAVICCHIA

Centro Euro-Mediterraneo sui Cambiamenti Climatici, Bologna, Italy

HANS VON STORCH

Institute for Coastal Research, Helmholtz-Zentrum Geesthacht, Geesthacht, Germany

SILVIO GUALDI

Centro Euro-Mediterraneo sui Cambiamenti Climatici, and Istituto Nazionale di Geofisica e Vulcanologia, Bologna, Italy

(Manuscript received 9 May 2014, in final form 15 July 2014)

ABSTRACT

The Mediterranean has been identified as one of the most responsive regions to climate change. It has been conjectured that one of the effects of a warmer climate could be to make the Mediterranean Sea prone to the formation of hurricanes. Already in the present climate regime, however, a few of the numerous low pressure systems that form in the area develop a dynamical evolution similar to the one of tropical cyclones. Even if their spatial extent is generally smaller and the life cycle shorter compared to tropical cyclones, such storms produce severe damage on the highly populated coastal areas surrounding the Mediterranean Sea. This study, based on the analysis of individual realistically simulated storms in homogeneous long-term and high-resolution data from multiple climate change scenarios, shows that the projected effect of climate change on Mediterranean tropical-like cyclones is decreased frequency and a tendency toward a moderate increase of intensity.

1. Introduction

It is known since the early times of meteorology (Meteorological Office 1937) that the Mediterranean Sea, because of its peculiar features, such as the interplay of the complex topography and orography and the geographical location between the subtropics and midlatitudes, is characterized by the formation of a large number of low pressure systems (Trigo and Davies 1999), mostly baroclinic in nature (Trigo et al. 2002). It has been suggested that the increased sea surface temperature in an anthropogenically warmed climate could lead to favorable conditions for the formation of hurricanes in the Mediterranean Sea (Gaertner et al. 2007). After the advent of satellite meteorology in the last decades of the twentieth century, on the other hand, evidence emerged (Ernst and Matson 1983; Rasmussen and Zick 1987) indicating that a few mesoscale vortices showing a striking resemblance to tropical latitude hurricanes occasionally do occur over the Mediterranean Sea. Such storms exhibit a cloud structure characterized by a central eye surrounded by spiral-shaped cloud bands, and the strong winds associated can reach hurricane strength; the most intense storms of this kind have thus been termed Mediterranean hurricanes (medicanes). The limited available observations of the atmospheric fields around medicanes (Pytharoulis et al. 2000; Reale and Atlas 2001; Moscatello et al. 2008; Lagouvardos et al. 1999) showed further similarities between their dynamical features and the ones of tropical cyclones: a warm core, a symmetric vertical profile, and rotating winds with a well-defined structure around the cyclone eye.

Theoretical (Emanuel 2005) and modeling (Davolio et al. 2009; Fita et al. 2007; Miglietta et al. 2013) studies investigating the mechanisms driving the formation of medicanes pointed out that the genesis of such cyclones is often characterized by the presence of cold air in the upper-atmospheric layers, associated with a cutoff low over the Mediterranean area. Similar atmospheric configurations

Corresponding author address: Leone Cavicchia, Centro Euro-Mediterraneo sui Cambiamenti Climatici, Viale Aldo Moro 44, 40127 Bologna, Italy.
E-mail: leone.cavicchia@cmcc.it

DOI: 10.1175/JCLI-D-14-00339.1

act as an important factor to enhance the atmospheric instability to a level high enough to trigger the formation of medicanes, which can occur above waters with surface temperatures substantially lower than the ones of tropical oceans (Miglietta et al. 2011; Palmén 1948).

The small scale and low frequency of medicanes hinders the systematic assessment of their properties in studies exploiting data derived from reanalysis or long-term climate model experiments that have a too coarse spatial resolution. Satellite-based detection, on the other hand, faces difficulties in reliably distinguishing such cyclones from baroclinic vortices.

A method based on the dynamical downscaling of global reanalysis data in a high-resolution atmospheric regional model, making use of the spectral nudging technique (von Storch et al. 2000), has been proven effective in successfully reproducing a number of historical medicane cases (Cavicchia and von Storch 2012). Such a method has been used in Cavicchia et al. (2014) to reconstruct the climatology of medicanes over the period 1948–2010.

In the present work we extend the aforementioned dynamical downscaling method to study the properties of all Mediterranean tropical-like cyclones (MTLCs) including, besides the most intense medicanes, weaker tropical-like storms. The same method is then applied to future climate scenarios, to estimate the response to climate change of the frequency and intensity of Mediterranean tropical-like cyclones.

2. Methods

The climatological properties of MTLCs over the last six decades are assessed by downscaling the National Centers for Environmental Prediction–National Center for Atmospheric Research (NCEP–NCAR) reanalysis data (Kalnay et al. 1996). To estimate the effect of climate change, we performed the downscaling of two different 30-yr (2070–99) time slices of climate scenarios produced by the global circulation model ECHAM5/Max Planck Institute Ocean Model (MPI-OM) (Roeckner et al. 2003) forced by the greenhouse gas concentrations prescribed in the Intergovernmental Panel on Climate Change (IPCC) Special Report on Emissions Scenarios (SRES) for emissions scenarios A2 and B1. To minimize the effect of systematic biases of the global model chosen, we also performed the downscaling of a 30-yr (1960–89) time slice of a present climate simulation produced by the same ECHAM5/MPI-OM global circulation model, forced by twentieth-century greenhouse gases concentrations (C20 simulation); the scenario simulations are thus compared with the control run. The dynamical downscaling of atmospheric fields is performed using the limited-area model the Consortium for Small-Scale Modeling in Climate Mode (COSMO-CLM; Rockel et al. 2008). The model features nonhydrostatic equations and has 32 vertical sigma levels. Boundary and initial conditions are obtained by the NCEP–NCAR reanalysis or by the global circulation model ECHAM5/MPI-OM. The regional model is run at 0.09° (~10 km) horizontal resolution on a domain of 386 × 206 grid points covering the whole Mediterranean Sea and the main mountain ranges around it. The model is run in a double-nested configuration, with an intermediate integration on a 0.22° (~25 km) grid on a domain of 176 × 106 grid points; only the final 10-km-resolution simulation is used for the analysis. The atmospheric fields produced by the model are saved every hour, on 19 pressure levels ranging between 1000 and 100 hPa at evenly spaced 50-hPa intervals. Spectral nudging (von Storch et al. 2000) is applied on the horizontal components of the wind field components for spatial scales larger than approximately 4 times the grid size of the forcing fields and on vertical levels above 850 hPa, while the small-scale components and the lower vertical levels are let free to evolve following the small-scale dynamics and high-resolution orography.

All the storms exhibiting tropical-like features are detected in the four downscaled simulations, using an objective detection algorithm specifically designed for MTLCs. The geographical distribution, seasonal cycle, and intensity distribution of the detected storms are then compared. The detection algorithm consists of the following steps. The sea level pressure minima with a gradient larger than 20 Pa over three grid points are assigned to the same track if they lie within a radius of 100 km at two consecutive hourly time steps. The tracks composed of at least six points are kept for further analysis if the following occurs: no more than half of the positions correspond to land-covered model grid points, the two most distant positions are separated by at least 200 km, and a change in the propagation direction does not exceed $\pi/3$ for more than half of the positions. A cyclone is classified as an MTLC if for more than 10% of the track or more than 6 h the following occurs: it is positioned in the symmetric and warm core sector of the phase space defined in Hart (2003) with a radius of 100 km, the 10-m wind speed within a 50-km radius around the pressure minimum exceeds 18 m s^{-1}, and its average is larger at 850 hPa than at 300 hPa. A sensitivity analysis to the numerical values of the different parameters entering the detection algorithm, and the validation and optimization procedure employed to determine the thresholds described above, have been presented and discussed in a previous work (Cavicchia et al. 2014).

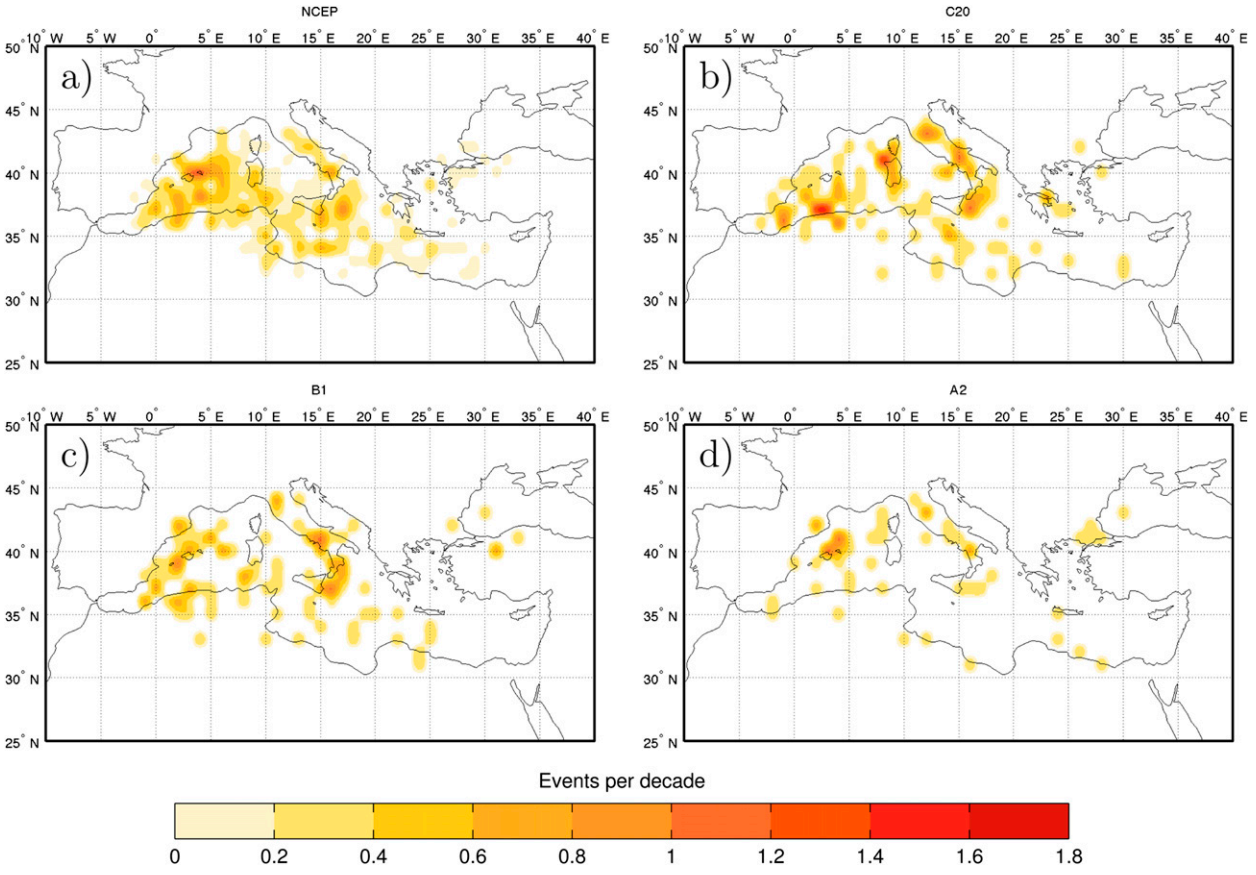

FIG. 1. Genesis density of MLTCs (first location in the track) per 1° × 1° box per decade: (a) NCEP, (b) C20, (c) B1, and (d) A2.

3. Results

a. Statistical properties of MTLCs

The locations of formation (Fig. 1) of all the MTLCs detected in the reanalysis-driven downscaling show a pattern characterized by two maxima located in the western Mediterranean and in the Ionian Sea, and very low activity in the eastern Mediterranean. Such a formation pattern is similar to the one found in Cavicchia et al. (2014) for the subset of the stronger medicanes;[1] on the other hand, including the full set of MTLCs the frequency is increased about 3 times with respect to the one found for medicanes. A comparison with the limited satellite-based observations available (Fita 2014) and modeling studies (Walsh et al. 2014; Romero and Emanuel 2013) using different methodology and data shows similar patterns. The C20 simulation produces a consistent formation pattern, with most of the events produced in the western Mediterranean and a secondary maximum in the Ionian Sea; a few minor differences in the exact location of the cyclogenesis maxima are, however, visible. On the other hand, the overall frequency of detected MTLCs in the C20 simulation is about 20% lower compared to the one found in the NCEP downscaling. Such discrepancy is due to the bias in the atmospheric variables on which MTLC formation depends, mostly the vertical temperature gradient controlling the atmospheric stability. The role of vertical temperature gradients in the formation of Mediterranean tropical-like cyclones is discussed in detail in section 3b below; it is, however, anticipated that the C20 simulation shows a negative bias in the amplitude of the temperature difference between the high troposphere and sea surface ranging between 1° and 2°C with respect to the NCEP-driven simulation in the areas of MTLC formation (see Fig. 5e).

In the B1 simulation, the MTLC formation rate shows a moderate reduction (about 15%) compared to C20. A few small-scale changes in the locations of formation are visible (e.g., the maximum west of Sardinia); the decrease

[1] Following Cavicchia et al. (2014), MTLCs are classified as medicanes if the track fulfills the additional criterion to have a value of the peak wind speed V_{MAX} larger than 29 m s^{-1} for at least 4 h.

TABLE 1. Total number of cyclones detected in the main subregions in the different simulations.

	NCEP	C20	B1	A2
Western (lon < 9°E)	124	48	43	23
Ionian (lat < 40.5°N; 16°E < lon < 22.5°E)	78	27	23	6
Eastern (lon > 22.5°E)	27	8	6	4

of the formation rate, however, is equal over the main different subregions (Table 1). In the A2 simulation, the decrease in frequency becomes substantial (about a 60% decrease with respect to C20). Moreover, the frequency of formation in the Ionian Sea area shows a strong decrease.

The seasonal cycle of cyclone formation in the four different experiments characterizes Mediterranean tropical-like storms as a cold season phenomenon (Fig. 2). The seasonal cycle, like the formation pattern, shows features similar to the ones found for medicanes only. The relative difference between the four simulations reflects, except for a number of minor fluctuations, the changes in the respective overall frequency. A noticeable shrinking of the formation season, however, emerges in the A2 simulation.

The intensity distribution of MTLCs (Fig. 3) is derived using as an intensity metric the maximum value in a 50-km radius around the pressure minimum of the V_{MAX}, during each storm lifetime. This variable has been shown, through validation with observations, to provide a good criterion to discriminate medicanes from weaker Mediterranean tropical-like storms (Cavicchia et al. 2014). Both the mean value of the intensity distribution and the percentile corresponding to storms exceeding the medicane intensity threshold (29 m s^{-1}) show (Table 2) an increase in the climate change simulations compared to the control run. Moreover, events reaching extreme ($\gtrsim$50 m s^{-1}) wind speeds are present in both scenario simulations, while the most intense event in the control simulation has a maximum peak wind speed of 43 m s^{-1}.

b. *Environmental factors associated with decreased frequency of storms*

To investigate the decreased frequency of cyclones detected in the scenario simulations, we analyzed a number of factors that have been shown in the literature (Cavicchia et al. 2014; Tous et al. 2013) to be related to the formation of MTLCs. Such factors include the vertical temperature gradient between the sea surface and the high troposphere $\Delta T = |T(350\,\text{hPa}) - \text{SST}|$, the vertically integrated humidity content of the atmosphere

$$\text{HI} = \sum_{l=100\,\text{hPa}}^{1000\,\text{hPa}} \text{RH}(l),$$

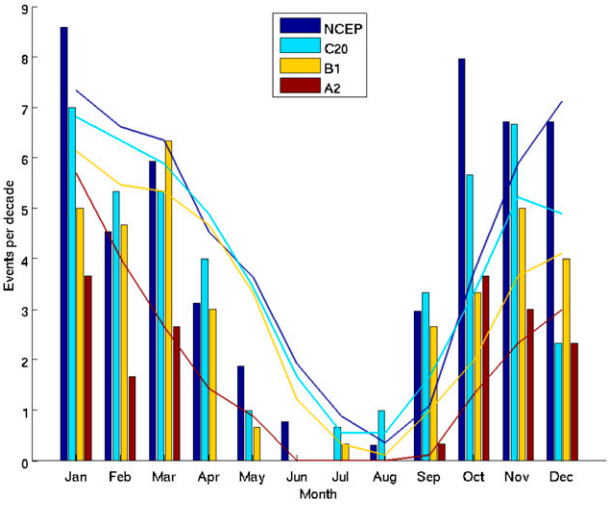

FIG. 2. Average number of MTLCs per month per decade (bars) and 3-month running mean (lines) in NCEP (blue), C20 (cyan), B1 (yellow), and A2 (red).

where RH represents relative humidity and the sum is calculated on the model output levels, evenly spaced at 50-hPa intervals, and the wind shear between the 850- and 250-hPa levels $\text{WS} = [(u_{250} - u_{850})^2 + (v_{250} - v_{850})^2]^{1/2}$. Adapting the approach used in Cavicchia et al. (2014) for the subset of most intense medicanes to the full set of Mediterranean tropical-like cyclones, we find that the detected MTLCs form when $\Delta T > 57$°C, HI > 1000, and WS < 18 m s^{-1}. We analyze, for each of the environmental variables WS, HI, and ΔT, the changes in future climate simulations of the mean state and of the percentage of days in which the threshold corresponding to MTLC formation is exceeded. We consider only the cold season, averaging the model variables over the months from October to March (ONDJFM). The exceedance probabilities are obtained from the model daily mean fields, calculating for every grid point the quantity $\mathcal{P}(V) = 100\ \text{ND}(V > \mathcal{T})/\text{ND}_{\text{TOT}}$, where ND is the number of days in which the variable V has a value larger than the threshold value $\mathcal{T}$ and ND_{TOT} is the total number of days in the simulation. For the changes in the mean state, we consider the relative difference $100(\overline{V}_{\text{B1,A2}} - \overline{V}_{\text{C20}})/\overline{V}_{\text{C20}}$.

The frequency of all environmental configurations favorable for MTLC formation shows a coherent decrease in both future climate scenarios. The magnitude and pattern of the change of the three analyzed factors is different.

The cold season mean state of WS in the C20 simulation ranges between 22 and 24 m s^{-1} in the western part of the basin; in the eastern Mediterranean, it shows larger values, up to 36 m s^{-1}, with a southeastward gradient. The mean state of the wind shear during the cold season is increased in warmer climates. The magnitude of the

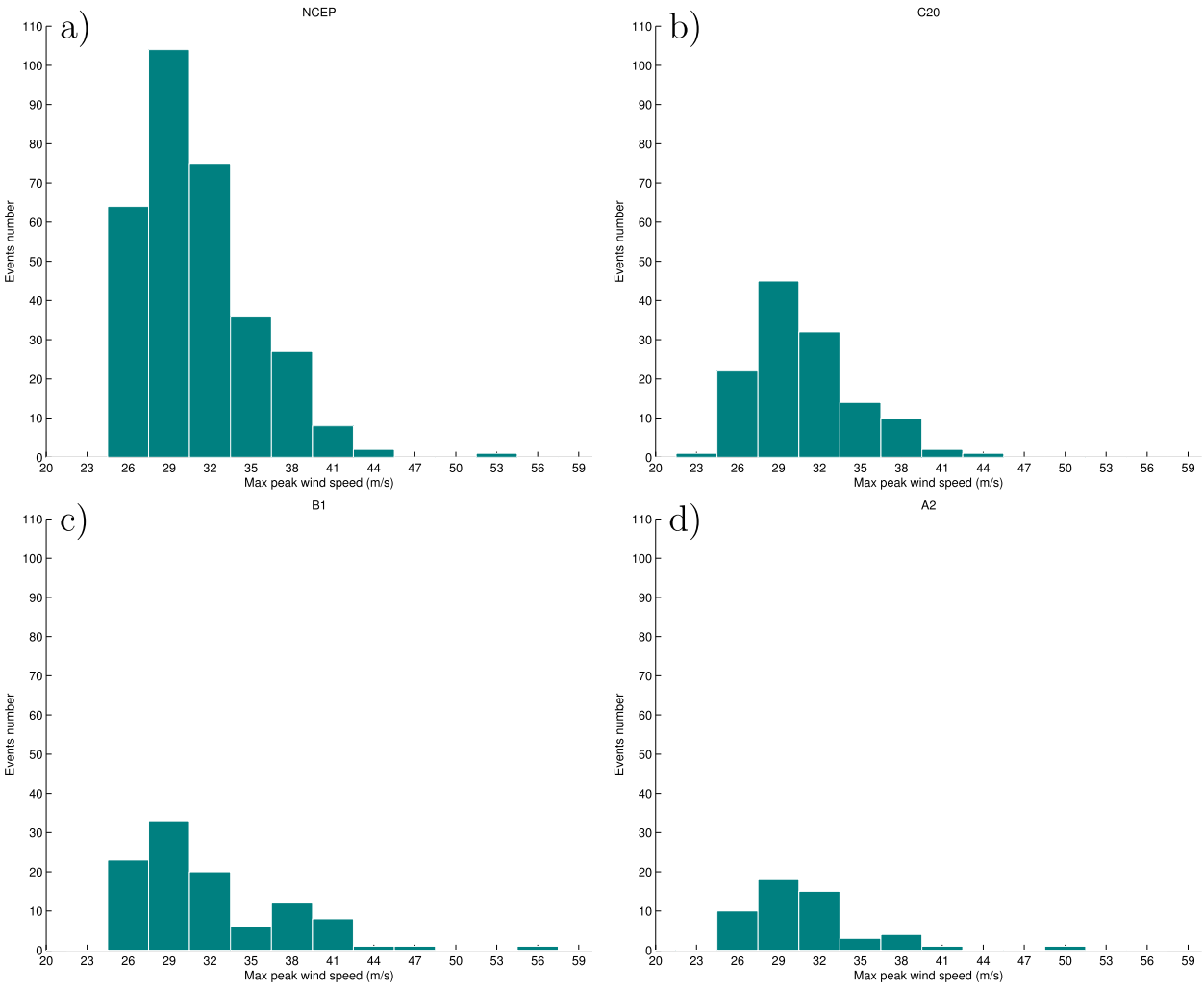

FIG. 3. The maximum value of V_{MAX} detected in a 50-km radius during the storm lifetime for (a) NCEP, (b) C20, (c) B1, (d) A2. Bins represent $3\,m\,s^{-1}$ intervals centered at the values indicated on the x axis. The lower bound at around $25\,m\,s^{-1}$ in V_{MAX} is due to the $18\,m\,s^{-1}$ cutoff applied to the average wind speed in the detection algorithm (see section 2).

relative increase is, in the areas of MTLC formation, 3%–5% in the B1 scenario (not shown) and 5%–10% in the A2 scenario (Fig. 4a), while it remains unchanged in the southern part of the basin. The frequency of configurations with wind shear low enough for MTLC formation ($WS < 18\,m\,s^{-1}$) shows a moderate decrease in the same area of about 2% in the B1 scenario (not shown) and 4% in the A2 scenario (Fig. 4b).

The cold season mean state of the integrated relative humidity is characterized in the C20 simulation by a strong meridional gradient, being about 3 times lower in the southern Mediterranean compared to the northern part of the basin. The HI mean state shows a moderate relative decrease in the areas of MTLC formation of 3% in B1 (not shown) and 5% in A2 (Fig. 4c), with the larger difference in the southeastern Mediterranean.

TABLE 2. Summary of the main statistical properties of detected MTLCs.

	NCEP	C20	B1	A2
Sample size	317	127	105	52
Frequency (events per year)	3.91 ± 1.85	3.26 ± 2.02	2.68 ± 1.33	1.35 ± 1.17
Mean intensity ($m\,s^{-1}$)	31.01 ± 4.09	30.79 ± 3.83	31.77 ± 5.40	31.13 ± 4.25
$29\,m\,s^{-1}$ intensity percentile	63.09	63.78	63.81	67.32

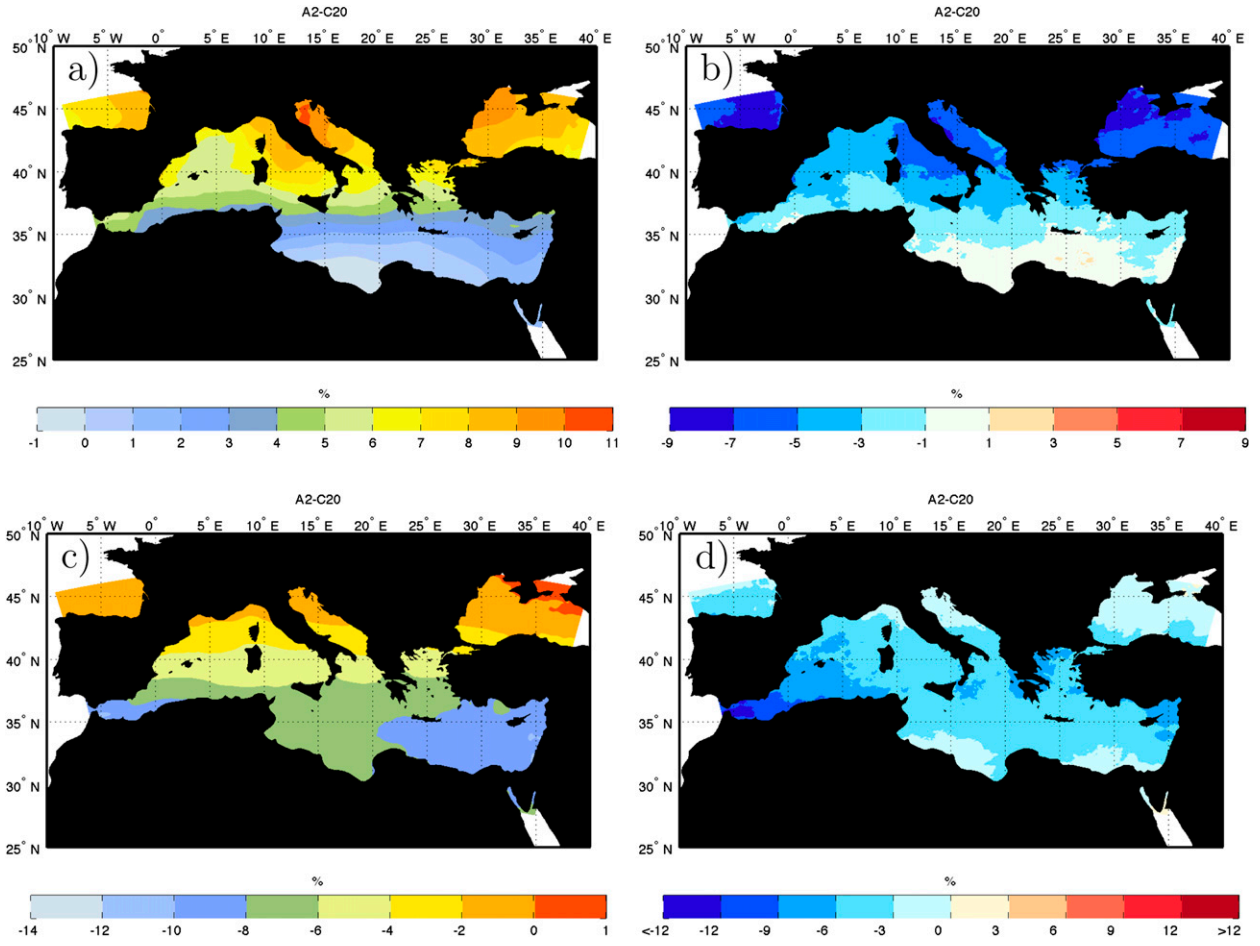

FIG. 4. Changes in large-scale parameters related to MTLC formation in future climate scenarios. (a) Mean value of wind shear in the cold season (ONDJFM), relative difference between the A2 and C20 scenarios. (b) Frequency of days with WS $< 18\,\mathrm{m\,s^{-1}}$, difference between the A2 and C20 scenarios. (c) As in (a), but for relative humidity. (d) Frequency of days with HI > 1000, difference between the A2 and C20 scenarios.

The frequency of configurations with atmospheric humidity high enough for MTLC formation (HI > 1000) shows a comparable decrease in the scenario simulations, of about 3% in B1 (not shown) and 5% in A2 (Fig. 4d).

The major change between present and future climate is found in the vertical atmospheric temperature gradient. The probability of atmospheric configurations with ΔT high enough for MTLC formation ($\Delta T > 57$°C) shows a decrease in the central Mediterranean of about 13%–15% in the B1 scenario (Fig. 5b) and of 19%–21% in the A2 scenario (Fig. 5d). The realization of a given value of the vertical temperature gradient ΔT can be written as $\Delta T = \overline{\Delta T} - \tilde{T} + \tilde{S}$, where $\overline{\Delta T}$ represents the mean state of the temperature gradient, $\tilde{T} = T - \overline{T}$ is the deviation of the 350-hPa temperature from its mean state, and $\tilde{S} = S - \overline{S}$ is the deviation of the sea surface temperature from its mean state. It was found in Cavicchia et al. (2014) that the formation of medicanes is driven by the factor $\tilde{T}$, whereas $\tilde{S}$ does not show a coherent signal associated with the formation of medicanes. It is worth disentangling the effect of the two remaining factors—the mean value of the temperature difference $\overline{\Delta T}$ and the frequency of cold anomalies $\tilde{T}$ in the high troposphere—whose combination contributes to reaching the value of instability needed for the formation of MTLCs, since they can be influenced differently by climate change. The mean value $\overline{\Delta T}$ decreases about 2°C, or 3%, in B1 (Fig. 5a) and 3°C, or 5%, in A2 (Fig. 5c), with a larger difference in the central part of the basin. Such a decrease reflects the fact that the atmosphere responds faster than ocean to climate warming (Collins 2014). The increase of the mean value of sea surface temperature in the A2 scenario is shown in Fig. 5f. The frequency of cold anomalies $\tilde{T}$ of the 350-hPa temperature with respect to its mean value (Fig. 5g), on the other hand, shows a slight increase in the scenario simulations, for a fixed amount of the anomaly value. Since the mean value has changed, however, reaching the threshold associated with MTLC formation requires

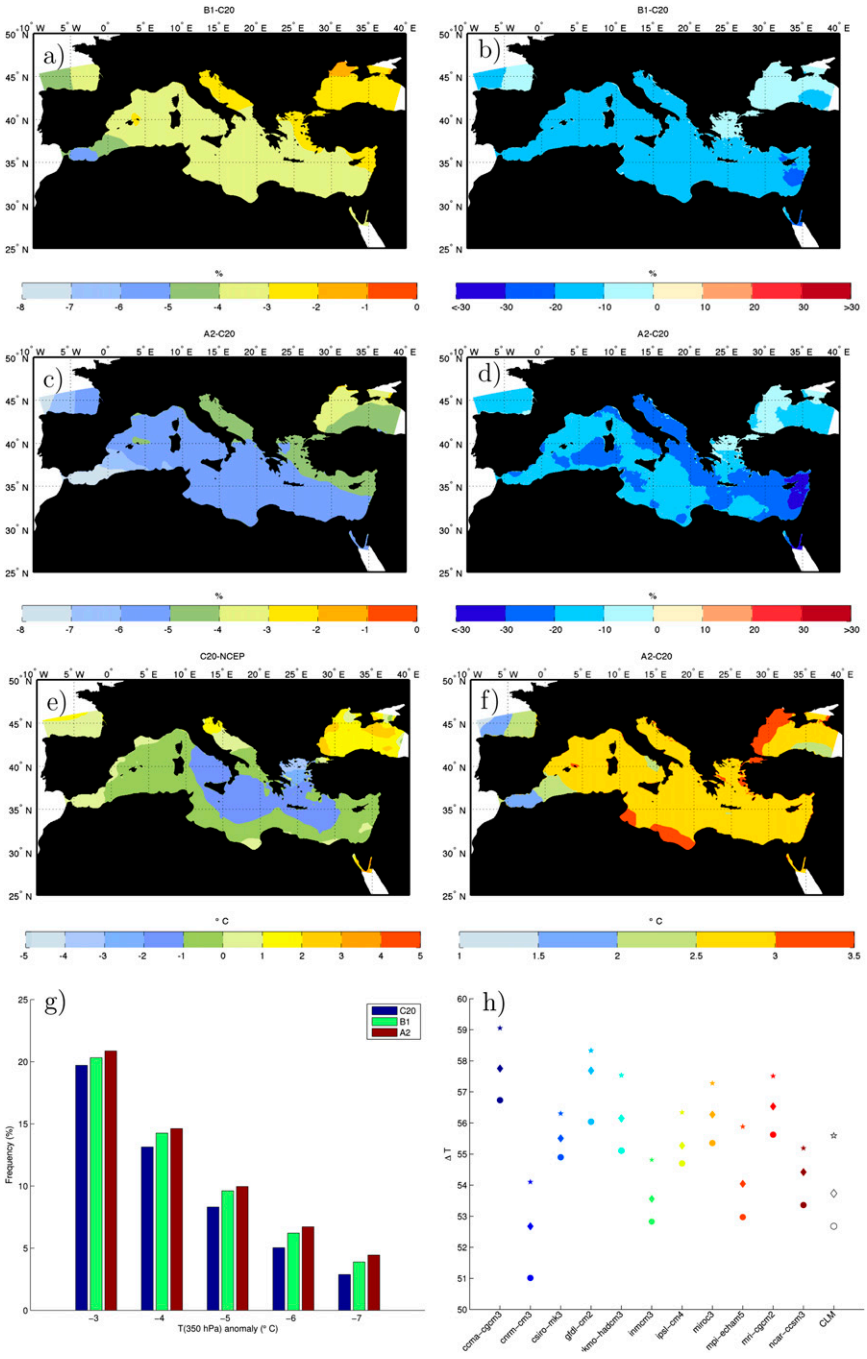

FIG. 5. Changes in the atmospheric temperature and MTLC formation in future climate scenarios. (a) Mean value of ΔT in the cold season (ONDJFM), relative difference between the B1 and C20 scenarios. (b) Frequency of days with $\Delta T > 57$°C, difference between the B1 and C20 scenarios. (c),(d) As in (a),(b), but for the A2 and C20 scenario difference.(e) Mean value of ΔT in the cold season, difference between the C20 and NCEP simulations. (f) Mean value of SST in the cold season, difference between the A2 and C20 scenarios. (g) Frequency of days (basin average, sea points only) with anomalies (with respect to the monthly climatological value) of T (350 hPa) larger than the value indicated on the x axis in C20 (blue), B1 (green), and A2 (red). (h) Mean value of ΔT (basin average, sea points only) in the cold season in different CMIP3 models and downscaled simulations in C20 (stars), B1 (diamonds), and A2 (circles).

a larger anomaly that is less frequent, and this explains the decreased probability of occurrence of values of ΔT above the threshold. The increased frequency of anomalies of equal amplitude in the scenario simulations is coherent with the expectation of a slower warming of the upper troposphere at high latitudes (Collins 2014), since cold anomalies are associated with the intrusion in the Mediterranean region of air masses originated in higher latitudes; the proof of such conjecture, however, goes beyond the scope of the present work. Summarizing the main results of the discussion, we find that (i) in a warmed climate, the mean temperature difference between the sea surface and the high troposphere is decreased, due to the atmosphere warming faster than the ocean; and (ii) the frequency of negative fluctuations of a given magnitude of the high troposphere temperature around the mean value remains mostly unchanged in a warmed climate; however, because of the decrease of the mean value, a larger anomaly is required to reach the threshold associated with cyclone formation, and this explains the reduced frequency of storms.

Finally, we compared the changes in the mean value of ΔT obtained in our simulations with the values obtained in a number of models from phase 3 of the Coupled Model Intercomparison Project (CMIP3; Meehl et al. 2007). The spread in the value of ΔT (Fig. 5h) reflects the different model biases, but the strength of the decrease found in the B1 and A2 scenarios is comparable in most of the models, increasing the confidence in the robustness of the projected changes in storm frequency.

4. Conclusions and outlook

Storms exhibiting dynamical features similar to the ones of tropical cyclones occur occasionally over the Mediterranean Sea. For a fraction of such storms, the tropical-like intensification is strong and long-lasting enough to allow them to attain hurricane strength. Different from tropical-latitude hurricanes, cold air aloft is required in order to enhance thermodynamic disequilibrium and trigger the formation of Mediterranean tropical-like cyclones. The formation of MTLCs is found to occur mostly in the central and western parts of the basin during the cold season. The frequency of MTLCs is projected to decrease in future climate scenarios, as a consequence of the lower frequency of environmental configurations favorable for their formation. The projected intensity of simulated MTLCs in scenario simulations shows on the other hand a tendency to a moderate increase. The robust assessment of changes in MTLC intensity requires, however, further investigation based on a larger sample of simulated events, and on the analysis of the physical mechanisms involved in MTLC intensification.

Acknowledgments. We acknowledge the modeling groups the Program for Climate Model Diagnosis and Intercomparison (PCMDI) and the WCRP's Working Group on Coupled Modelling (WGCM) for their roles in making available the WCRP CMIP3 multimodel dataset. Support of this dataset is provided by the Office of Science, U.S. Department of Energy. L. C. was partially supported by the NextData project, funded by the Italian Ministry of Education, Universities and Research.

REFERENCES

Cavicchia, L., and H. von Storch, 2012: The simulation of medicanes in a high-resolution regional climate model. *Climate Dyn.,* **39,** 2273–2290, doi:10.1007/s00382-011-1220-0.

——, ——, and S. Gualdi, 2014: A long-term climatology of medicanes. *Climate Dyn.,* **43,** 1183–1195, doi:10.1007/s00382-013-1893-7.

Collins, M., and Coauthors, 2014: Long-term climate change: Projections, commitments and irreversibility. *Climate Change 2013: The Physical Science Basis,* T. F. Stocker et al., Eds., Cambridge University Press, 1029–1136. [Available online at http://www.climatechange2013.org/images/report/WG1AR5_Chapter12_FINAL.pdf.]

Davolio, S., M. M. Miglietta, A. Moscatello, F. Pacifico, A. Buzzi, and R. Rotunno, 2009: Numerical forecast and analysis of a tropical-like cyclone in the Ionian Sea. *Nat. Hazards Earth Syst. Sci.,* **9,** 551–562, doi:10.5194/nhess-9-551-2009.

Emanuel, K., 2005: Genesis and maintenance of ''Mediterranean hurricanes.'' *Adv. Geosci.,* **2,** 217–220, doi:10.5194/adgeo-2-217-2005.

Ernst, J. A., and M. Matson, 1983: A Mediterranean tropical storm? *Weather,* **38,** 332–337, doi:10.1002/j.1477-8696.1983.tb04818.x.

Fita, L., cited 2014: Medicanes: Mediterranean tropical-like storms. [Available online at http://www.uib.es/depart/dfs/meteorologia/METEOROLOGIA/MEDICANES.]

——, R. Romero, A. Luque, K. Emanuel, and C. Ramis, 2007: Analysis of the environments of seven Mediterranean tropical-like storms using an axisymmetric, nonhydrostatic, cloud resolving model. *Nat. Hazards Earth Syst. Sci.,* **7,** 41–56, doi:10.5194/nhess-7-41-2007.

Gaertner, M., D. Jacob, V. Gil, M. Domínguez, E. Padorno, E. Sánchez, and M. Castro, 2007: Tropical cyclones over the Mediterranean Sea in climate change simulations. *Geophys. Res. Lett.,* **34,** L14711, doi:10.1029/2007GL029977.

Hart, R. E., 2003: A cyclone phase space derived from thermal wind and thermal asymmetry. *Mon. Wea. Rev.,* **131,** 585–616, doi:10.1175/1520-0493(2003)131<0585:ACPSDF>2.0.CO;2.

Kalnay, E., and Coauthors, 1996: The NCEP/NCAR 40-Year Reanalysis Project. *Bull. Amer. Meteor. Soc.,* **77,** 437–471, doi:10.1175/1520-0477(1996)077<0437:TNYRP>2.0.CO;2.

Lagouvardos, K., V. Kotroni, S. Nickovic, D. Jovic, G. Kallos, and C. J. Tremback, 1999: Observations and model simulations of a winter sub-synoptic vortex over the central Mediterranean. *Meteor. Appl.,* **6,** 371–383, doi:10.1017/S1350482799001309.

Meehl, G. A., C. Covey, K. E. Taylor, T. Delworth, R. J. Stouffer, M. Latif, B. McAvaney, and J. F. B. Mitchell, 2007: The WCRP CMIP3 multimodel dataset: A new era in climate change research. *Bull. Amer. Meteor. Soc.,* **88,** 1383–1394, doi:10.1175/BAMS-88-9-1383.

Meteorological Office, 1937: *Weather in the Mediterranean.* Vol. 1, *General Meteorology,* Her Majesty's Stationery Office, 218 pp.

Miglietta, M. M., A. Moscatello, D. Conte, G. Mannarini, G. Lacorata, and R. Rotunno, 2011: Numerical analysis of a Mediterranean 'hurricane' over southeastern Italy: Sensitivity experiments to sea surface temperature. *Atmos. Res.,* **101,** 412–426, doi:10.1016/j.atmosres.2011.04.006.

——, S. Laviola, A. Malvaldi, D. Conte, V. Levizzani, and C. Price, 2013: Analysis of tropical-like cyclones over the Mediterranean Sea through a combined modelling and satellite approach. *Geophys. Res. Lett.,* **40,** 2400–2405, doi:10.1002/grl.50432.

Moscatello, A., M. M. Miglietta, and R. Rotunno, 2008: Observational analysis of a Mediterranean 'hurricane' over southeastern Italy. *Weather,* **63,** 306–311, doi:10.1002/wea.231.

Palmén, E., 1948: On the formation and structure of tropical hurricanes. *Geophysica,* **3,** 26–38.

Pytharoulis, I., G. Craig, and S. Ballard, 2000: The hurricane-like Mediterranean cyclone of January 1995. *Meteor. Appl.,* **7,** 261–279, doi:10.1017/S1350482700001511.

Rasmussen, E., and C. Zick, 1987: A subsynoptic vortex over the Mediterranean with some resemblance to polar lows. *Tellus,* **39A,** 408–425, doi:10.1111/j.1600-0870.1987.tb00318.x.

Reale, O., and R. Atlas, 2001: Tropical cyclone–like vortices in the extratropics: Observational evidence and synoptic analysis. *Wea. Forecasting,* **16,** 7–34, doi:10.1175/1520-0434(2001)016<0007:TCLVIT>2.0.CO;2.

Rockel, B., A. Will, and A. Hense, 2008: The regional climate model COSMO-CLM (CCLM). *Meteor. Z.,* **17,** 347–348, doi:10.1127/0941-2948/2008/0309.

Roeckner, E., and Coauthors, 2003: The atmospheric general circulation model ECHAM 5. Part I: Model description. MPI Rep. 349, 140 pp. [Available online at http://www.mpimet.mpg.de/fileadmin/publikationen/Reports/max_scirep_349.pdf.]

Romero, R., and K. Emanuel, 2013: Medicane risk in a changing climate. *J. Geophys. Res. Atmos.,* **118,** 5992–6001, doi:10.1002/jgrd.50475.

Tous, M., R. Romero, and C. Ramis, 2013: Surface heat fluxes influence on medicane trajectories and intensification. *Atmos. Res.,* **123,** 400–411, doi:10.1016/j.atmosres.2012.05.022.

Trigo, I. F., and T. D. Davies, 1999: Objective climatology of cyclones in the Mediterranean region. *J. Climate,* **12,** 1685–1696, doi:10.1175/1520-0442(1999)012<1685:OCOCIT>2.0.CO;2.

——, ——, and G. R. Bigg, 2002: Climatology of cyclogenesis mechanisms in the Mediterranean. *Mon. Wea. Rev.,* **130,** 549–569, doi:10.1175/1520-0493(2002)130<0549:COCMIT>2.0.CO;2.

von Storch, H., H. Langenberg, and F. Feser, 2000: A spectral nudging technique for dynamical downscaling purposes. *Mon. Wea. Rev.,* **128,** 3664–3673, doi:10.1175/1520-0493(2000)128<3664:ASNTFD>2.0.CO;2.

Walsh, K., F. Giorgi, and E. Coppola, 2014: Mediterranean warm-core cyclones in a warmer world. *Climate Dyn.,* **42,** 1053–1066, doi:10.1007/s00382-013-1723-y.